Bioorganic & Medicinal Chemistry 18 (2010) 2173–2177

Contents lists available at ScienceDirect

Bioorganic & Medicinal Chemistry

journal homepage: www.elsevier.com/locate/bmc

Acetylcholinesterase inhibitors from the toadstool *Cortinarius infractus*

Torsten Geissler [a], Wolfgang Brandt [a], Andrea Porzel [a], Dagmar Schlenzig [b], Astrid Kehlen [b], Ludger Wessjohann [a], Norbert Arnold [a,*]

[a] *Department of Bioorganic Chemistry, Leibniz Institute of Plant Biochemistry, Weinberg 3, D-06120 Halle (Saale), Germany*
[b] *Probiodrug AG, Weinbergweg 22, D-06120 Halle (Saale), Germany*

ARTICLE INFO

Article history:
Received 30 September 2009
Revised 22 January 2010
Accepted 22 January 2010
Available online 4 February 2010

Keywords:
Alzheimer's disease
β-Carbolines
Fungi
Docking studies

ABSTRACT

Inhibition of acetylcholinesterase (AChE) and therefore prevention of acetylcholine degradation is one of the most accepted therapy opportunities for Alzheimeŕs disease (AD), today. Due to lack of selectivity of AChE inhibitor drugs on the market, AD-patients suffer from side effects like nausea or vomiting. In the present study the isolation of two alkaloids, infractopicrin (**1**) and 10-hydroxy-infractopicrin (**2**), from *Cortinarius infractus* Berk. (Cortinariaceae) is presented. Both compounds show AChE-inhibiting activity and possess a higher selectivity than galanthamine. Docking studies show that lacking π–π-interactions in butyrylcholinesterase (BChE) are responsible for selectivity. Studies on other AD pathology related targets show an inhibitory effect of both compounds on self-aggregation of Aβ-peptides but not on AChE induced Aβ-peptide aggregation. Low cytotoxicity as well as calculated pharmacokinetic data suggest that the natural products could be useful candidates for further drug development.

1. Introduction

Alzheimeŕs disease (AD) is one of the most common forms of dementia affecting predominantly elderly people. One aspect of the illness is that patients suffer from an impaired memory due to deposition of aggregated Aβ-peptides forming amyloid plaques. According to the cholinergic hypothesis these amyloid plaques are responsible for the cholinergic dysfunctions in the brains of AD-patients.[1] The currently most accepted therapy is the application of mild and reversible acetylcholinesterase (AChE) inhibitors to restore acetylcholine levels and therefore cholinergic brain activity. Another process discussed in this context is a catalytic role of the peripheral anionic site of AChE as catalyst for plaque formation from Aβ-peptides.[2] Butyrylcholinesterase (BChE), a close relative of AChE has a similar active site but a distinct periphery, hence it is less prone to catalyze amyloid plaque formation.[3] Probably due to insufficient selectivity of today's available AChE-inhibitors AD-patients suffer from side effects like nausea or vomiting, which are possibly ascribed to undesirable BChE-inhibition.[4,5] Additionally, bioavailability problems as well as slow pharmacokinetics create a demand for new and selective AChE-inhibitors. Natural sources provide a fascinating variety of structurally distinct and biologically active secondary metabolites. Especially secondary metabolites from plant origin show significant AChE inhibitory activity and may be relevant for AD therapy.

In contrast to plants, fungal fruiting bodies (macromycetes) are still widely untapped with regard to bioprospecting for new drugs or treatments, for example, AD. It is estimated that up to 1.5 million different fungi (Eumycota) exist, of which only approximately 7–8% are known to science yet.[6] Some groups of macromycetes yield an enormous diversity of pigments and bioactive secondary metabolites.[7,8] Most of these metabolites are not found outside of the fungal kingdom, therefore fungi constitute a valuable complementary source for novel lead compounds.

This article describes the bioassay-guided isolation and structure elucidation of the new indole alkaloid derivative 10-hydroxy-infractopicrin (**2**) from fruiting bodies of *Cortinarius infractus* Berk. (Cortinariaceae). Together with infractopicrin (**1**)[9] it is shown to have inhibitory activity against AChE whilst having low cytotoxicity. Docking studies of both compounds **1** and **2** give hints on their binding mode.

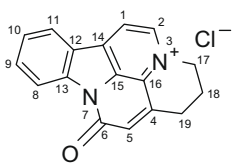

1 **2**

2. Results and discussion

The AChE inhibitory effects were tested according to Ellman's method.[10] For active compounds **1** and **2**, IC_{50}-values were determined by fitting the percentage of inhibition to a sigmoidal dose–response model using a variable Hill-Slope. To determine

* Corresponding author.
E-mail address: narnold@ipb-halle.de (N. Arnold).

0968-0896/$ - see front matter © 2010 Elsevier Ltd. All rights reserved.
doi:10.1016/j.bmc.2010.01.074

the esterase-selectivity of the isolated compounds, inhibition of BChE was also tested. For referencing, IC_{50}-values of known AChE-inhibitors were determined as well. Therefore, physostigmine, tacrine as well as the approved drug galanthamine, showing the highest AChE-selectivity of known pharmaceuticals,[11] were analyzed. It was observed that **1** and **2** show IC_{50}-values for AChE in a similar range as galanthamine (Table 1). However, for BChE no inhibition could be detected up to a concentration of 100 μM. This indicates an even higher esterase-selectivity of **1** and **2** (both >>10) compared to galanthamine (2.8; Table 1), although AChE and BChE inhibitory activity has been reported for other tricyclic β-carbolines.[12–14] In this context it is known that only β-carbolines and not their dihydro- and tetrahydroderivatives show activity on cholinesterases. Furthermore it is shown that the N3-alkylated β-carbolinium salts like **1** and **2** are the stronger inhibitors, possibly by substrate mimicking.[15] With respect to target selectivity it seems that β-carbolines are mostly AChE selective, with IC_{50}-ratios (AChE vs BChE) of up to 17.9 for the 6-hydroxy-9-methyl-norharmanium salt.[14] The compounds reported here show no inhibition of BChE at 100 μM hence their AChE-selectivity is suspected to be higher. Schott et al.[14] also speculate that AChE-selectivity is conferred by indole N-methylation. This is supported by the structures of compounds **1** and **2** where the indole nitrogen is amidated.

Additionally, the influence of the AChE-inhibitors on the aggregation of Aβ1-40 was investigated applying Thioflavin T(ThT) fluorescence assays. Incubation of monomeric Aβ1-40 with compound **1** or **2** in equimolar concentration resulted in a decreased maximum of ThT fluorescence (Fig. 1). This could be due to a reduced formation of fibrils or an influence of the compounds on fibril structure. A potential quenching of ThT fluorescence by the compounds **1** and **2** was investigated by incubation of mature fibrils of Aβ1-40 with the compounds. Only compound **1** exerted a minor quenching effect of about 15%, which efficiently ruled out an unspecific effect of the compounds on the fluorescence reading (Fig. 2). Thus, the reduced ThT fluorescence of about 50% in the aggregation assays in presence of the compounds is most likely caused by a reduction of the fibril concentration.

To confirm these results compounds **1** and **2** together with AChE were tested in a further Aβ1-40 aggregation assay (Fig. 4). This setup should demonstrate, if **1** and **2** interact only at the catalytic site or additionally at the peripheral site of AChE. As controls the site specific inhibitors tacrine (active site specific) and propidium iodide (peripheral site specific) were used. Inhibition of Aβ1-40 aggregation could be observed in the absence of AChE only. In conclusion, the alkaloids **1** and **2** inhibit only the self-aggregation of Aβ1-40 and not the aggregation induced by AChE. Therefore they can be seen as selective active site binders of AChE with no at most minor influence on the peripheral anionic site.

Table 1
Compounds **1** and **2** show similar IC_{50}-values for AChE compared with reference inhibitors, but due to not detectable inhibition of BChE a higher selectivity is indicated; figures show mean ± SEM

Compound	IC_{50} AChE (μM)	IC_{50} BChE (μM)	Selectivity (IC_{50} BChE/ IC_{50} AChE)
Galanthamine	8.70 ± 0.05	24.4 ± 2.84	2.80
Physostigmine	2.58 ± 0.03	1.34 ± 0.279	0.519
Tacrine	0.71 ± 0.30	0.01 ± 0.001	0.01
1	9.72 ± 0.19	No inhibition (100 μM)	>10
2	12.7 ± 0.16	No inhibition (100 μM)	>10

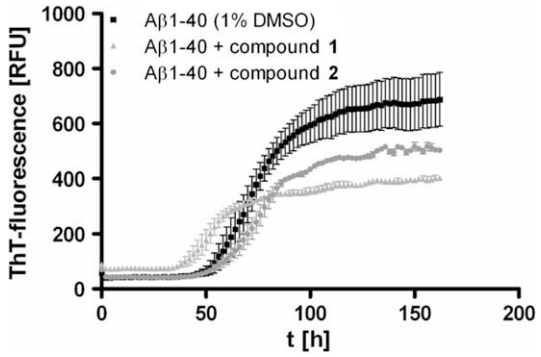

Figure 1. ThT fluorescence (λ_{exc} = 440 nm; λ_{emm} = 490 nm) during aggregation of Aβ1-40 (25 μM) in the presence of compounds **1** and **2** (both 25 μM). Maximum ThT fluorescence is reduced compared to control; figures show mean ± SEM.

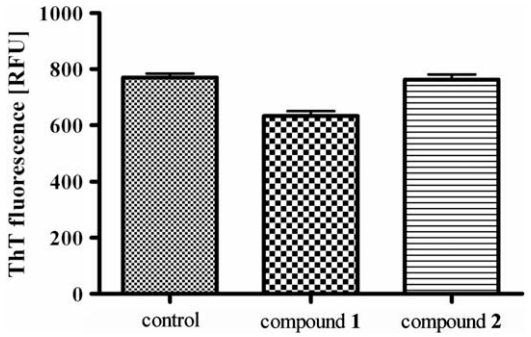

Figure 2. ThT fluorescence of Aβ1-40 fibrils in the presence of compound **1** and **2**. ThT fluorescence was quenched by compound **1** about 15%; bars show mean ± SEM.

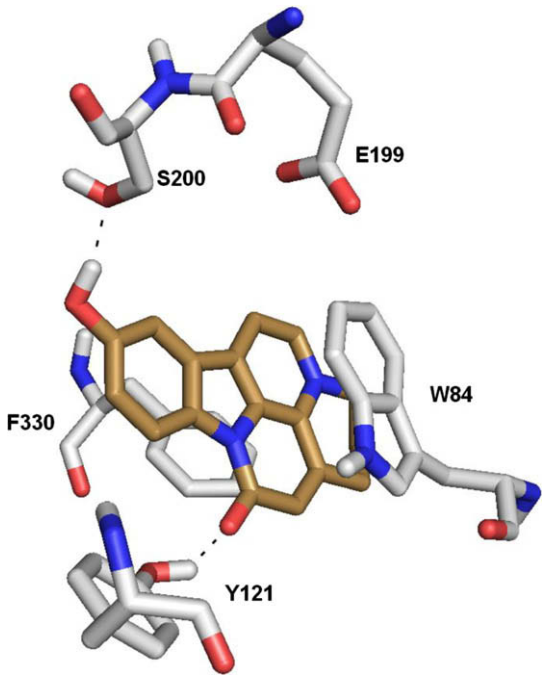

Figure 3. Cation π–π-interactions with W84 and F330 and hydrogen bond of the carbonyl group of the ligand with the phenolic hydroxy group of Y121. In case of the BChE-Q119 occupies the position of AChE-Y121. BChE-Q119 is neither in the right conformation for binding nor able to form π–π-interactions with the ligand. Even in flexible docking arrangements the side chain is too short to form the corresponding hydrogen bond. Furthermore, AChE-F330 is replaced by BChE-A328 which is not able to form π–π-interactions and to stabilize the docking arrangement. The negatively charged AChE-E199 electrostatically interacts with the positively charged ligand.

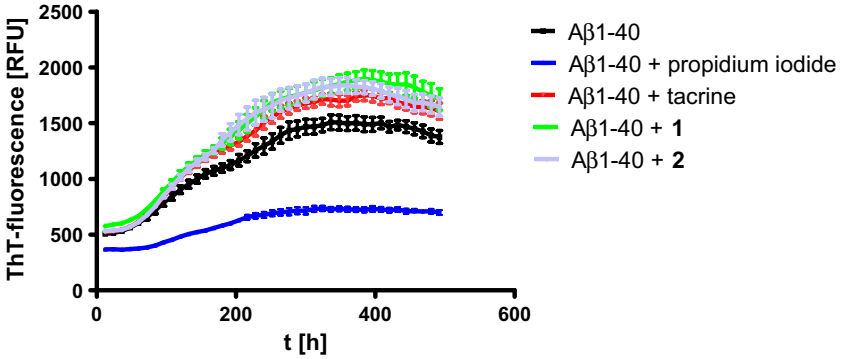

Figure 4. ThT fluorescence (λ_{exc} = 440 nm; λ_{emm} = 490 nm) during AChE induced aggregation of Aβ1-40 (25 μM) in the presence of compounds **1** and **2** as well as reference compounds (all 25 μM); figures show mean ± SEM.

After treatment for 24 h, no cytotoxic effects were observed for either compound **1** or **2** at concentrations up to 100 μM against four human cell lines including a neuroblastoma (SY5Y) and a hepatocyte cell line (HepG2). The viability of all cells was 100% (Table 4).

Moreover, calculated parameters indicate compliance of **1** and **2** with Lipinski's rules.[16,17] Calculated values for topological polar surface area (TPSA) below 70 Å^2 demonstrate that the substances could be able to diffuse through the blood-brain barrier[18] and therefore be active as CNS drug (Table 2).

To investigate the mechanism of a selective inhibition of AChE in detail, docking studies of the two inhibitors to AChE and BChE active sites were performed. For each ligand and enzyme, 30 docking arrangements were calculated. Those with best (more negative) scoring values were used for further discussions. Both compounds showed preferential binding to the oxyanion hole of the enzyme. In complex with AChE, stabilization occurs mainly by π–π-interactions with the aromatic residues W84 and F330. Furthermore, a hydrogen bond between the hydroxyl oxygen of Y121 and the carboxamide oxygen of the ligands fixes their positions (Fig. 3). An ion pair interaction of the quaternary nitrogen on the β-carboline moiety with the side chain of E199 could also be detected. The slightly better inhibition of **1** compared to its hydroxylated counterpart can be explained by an area of hydrophobic amino acids into which the hydroxyl group points. Interestingly, in the BChE complex none of the docking conformations produced by GOLD (Genetic Optimized Ligand Docking) or PLANTS (Protein–Ligand ANT System) was congruent with those from the AChE complex. In the BChE complex, the amino acids AChE-F330 and AChE-Y121 are replaced by A328 and Q119, which are not able to form π–π-interactions, responsible for the stabilization of the ligands in AChE. This can be an explanation for the selective inhibition of AChE by **1** and **2**. The formation of a hydrogen bond between the ligands carboxamide oxygen and the phenol-OH of Y121 is not possible in BChE. The ligand oxygen is 9.9 Å from the Y121 equivalent, Q119. Due to the decreased interaction possibilities in BChE, PLANTS produces different docking conformations with less ligand affinity towards BChE. This is also indicated by the scoring values which differ by 0.85–1.0, approximating the free interaction energy ΔG in kcal/mol between the ligand and the enzyme (Table 2). Due to the fact that the interaction energy is correlated logarithmic with the IC_{50}-value in the Gibbs–Helmholtz equation this translates into a difference of about one order of magnitude between the different enzymes (Table 2). Almost the same scoring difference was observed when docking the reference inhibitor galanthamine which has a lower AChE vs BChE selectivity than compounds **1** and **2** (Table 1).

The docking studies suggest possible reasons for the selectivity of **1** and **2** to the AChE active site versus BChE. Also in vitro fibril formation is positively influenced viz. reduced formation. Moreover, low cytotoxicity and the expected positive pharmacokinetic properties of the infractopicrin (**1**) scaffold make it a useful lead structure worth further investigations as AChE-inhibitors and consideration for the development as AD-drugs.

Table 2
PLANTS score values are normalized by the number of heavy atoms

Compound	PLANTS-Score AChE	PLANTS-Score BChE	*c*Log *P*	TPSA (Å^2)
1	−7.00	−5.95	3.179	25.88
2	−6.57	−5.73	2.885	46.11
Galanthamine	−5.93	−4.76	0.7	43.13

Higher affinity of the ligands to the enzyme is predicted for more negative PLANTS score values. *c*Log *P* and TPSA data indicate plasma membrane and blood-brain barrier permeability, respectively.
*c*Log *P* calculated octanol/water partion coefficient; TPSA topological polar surface area

Table 3
^{1}H and ^{13}C NMR data of compounds **1** and **2** (in D_2O)

Pos.	Infractopicrin (**1**)		10-Hydroxy-infractopicrin (**2**)	
	δ_C	δ_H m (*J* (Hz))	δ_C	δ_H m (*J* (Hz))
1	118.6	8.284 d (6.3)	118.7	8.400 d (6.3)
2	140.5	8.652 d (6.3)	140.3	8.846 d (6.3)
4	142.6		142.3	
5	128.2	6.814 t (1.8)	128.3	7.018 t (1.7)
6	158.7		158.4	
8	116.3	7.964 ddd (8.3, 1.0, 0.7)	117.2	7.893 d (8.8)
9	134.1	7.589 ddd (8.3, 7.5, 1.2)	121.5	7.086 dd (8.8, 2.4)
10	127.1	7.400 ddd (7.9, 7.5, 1.0)	154.8	
11	125.0	8.006 ddd (7.9, 1.2, 0.7)	109.8	7.405 d (2.4)
12	122.3		123.7	
13	140.9		134.8	
14	136.1		135.8	
15	132.0		132.2	
16	127.7		127.6	
17	54.3	4.727 m	54.4	4.925 m
18	21.5	2.335 m	21.5	2.537 m
19	24.1	3.009 m	24.1	3.206 m

Table 4
Cytotoxicity (LDH-activity) and viability of hepatocyte (HepG2) and neuroblastoma (SY5Y) cell lines against compounds **1** and **2**; figures show mean ± SEM

Compound	Concentration (μM)	Cytotoxicity SY5Y (%)	Cytotoxicity HepG2 (%)	Viability SY5Y (%)	Viability HepG2 (%)
1	10	−0.07 ± 0.25	2.23 ± 1.30	97.11 ± 1.94	100.45 ± 0.57
1	100	−1.33 ± 0.43	1.48 ± 0.85	97.66 ± 2.83	99.07 ± 0.39
2	10	−1.86 ± 1.67	0.13 ± 0.43	96.68 ± 7.92	98.65 ± 0.79
2	100	0.97 ± 0.54	0.56 ± 0.29	98.28 ± 0.53	100.74 ± 0.57

3. Experimental

3.1. General

UV spectra were obtained in MeOH on a Jasco V-560 spectrophotometer. IR spectra were measured on a Thermo Nicolet 5700 FT-IR spectrometer. 1D ^{1}H, ^{13}C, and 2D NMR spectra (HSQC, HMBC, COSY, ROESY) were recorded on a Varian Mercury 400 (^{1}H at 399.94 MHz) and on a Varian NMRS 600 (^{1}H at 599.83 MHz) spectrometer. ^{1}H and ^{13}C chemical shifts were referenced to external TSPSA in D_2O (δ 0.015 ppm, ^{1}H) and external dioxane in D_2O (δ 67.6 ppm, ^{13}C), respectively.

The LC/ESI-SRM measurements and the collision induced dissociation (CID) mass spectra were obtained from a TSQ Quantum Ultra AM system, equipped with a hot ESI source (HESI, electrospray voltage 3.0 kV, sheath gas: nitrogen; vaporizer temperature: 50 °C; capillary temperature: 250 °C). The MS system is coupled with a Surveyor Plus micro-HPLC (Thermo Electron), equipped with a RP18 column (5 μm, 150 × 1 mm, Hypersil GOLD, Thermo Scientific). For the HPLC, a gradient system was used starting from H_2O/CH_3CN 90:10 (each of them containing 0.2% HOAc) to 2:98 within 15 min and hold for further 30 min; flow rate 50 μl min^{-1} (collision gas: argon; collision pressure: 1.5 mTorr). The high-resolution ESI mass spectra were obtained from a Bruker Apex III Fourier Transform Ion Cyclotron Resonance (FT-ICR) mass spectrometer (Bruker Daltonics) equipped with an Infinity™ cell and a 7.0 Tesla superconducting magnet (Bruker). The dissolved and diluted probes were introduced via a continuously working syringe pump with a flow rate of 120 μ h^{-1}. TLC was carried out on aluminium TLC plates pre-coated with silica gel 60 F_{254} (Merck, 0.25 mm). Preparative HPLC was performed on a Varian ProStar 218 system with a PrepStar 330 photodiode array detector using an ODS C_{18} column (5 μm, 150 × 20 mm ID, YMC).

3.2. Fungal material

C. infractus Berk. was collected in a deciduous forest (*Carpinus, Fagus*, *Quercus*) near Bad Bibra, Saxony-Anhalt, Germany at 08.09.2006 (leg./det. N. Arnold, Koll. 08/2006). Voucher specimen is deposited at the Leibniz Institute of Plant Biochemistry Halle (Saale), Germany (IPB).

3.3. Extraction of fungal material and fractionation

The frozen fruiting bodies of *C. infractus* (318 g) were extracted with 3 L aqueous methanol (80%) at room temperature over night, and the resulting crude extract (8.43 g) was subjected to column chromatography on Diaion HP-20 eluting sequentially using the solvents H_2O (fraction 1) and MeOH (fraction 2).

3.4. Spectroscopic data

Only fraction 2 (MeOH eluate, 427 mg) showed AChE inhibition and was therefore purified by preparative HPLC equipped with a ODS C-18 column (eluents: H_2O and CH_3CN; solvent system: linear gradient: 0–43 min, 15–40% CH_3CN, flow rate of 8.0 mL min^{-1}) to afford compound **1** (R_t = 8.9 min) and **2** (R_t = 7.3 min). The constitution of **1** as infractopicrin was determined by detailed one- and two-dimensional NMR investigations and comparison of published spectroscopic data (^{1}H NMR, ^{13}C NMR, mass spectrometry).[9] Compound **2** was obtained as yellow solid. The UV spectrum exhibits absorption maxima at λ = 218, 235, 364, and 381 nm. The high-resolution MS shows a M^+-ion at *m/z* 277.09745 (calcd for $C_{17}H_{13}N_2O_2^+$, 277.09715) indicating in comparison with infractopicrin (**1**) an exchange of a proton by a hydroxy group. The ^{1}H NMR spectrum of **2** differs from **1** by the replacement of the aromatic four spin system by a three spin system because of an hydroxy substitution at the aromatic ring. Due to the observed NOE correlation between H-1 and the meta-coupled doublet at 7.405 ppm (H-11, d, ^{4}J = 2.5 Hz), the hydroxy group has to be attached to C-10. Thus, the structure of compound **2** was assigned as 10-hydroxy-infractopicrin (**2**). Based on the one- and two-dimensional NMR spectra of **1** and **2**, all ^{1}H and ^{13}C NMR signals were assigned unambiguously (Table 3).

Based on the frozen fungal raw material a yield of 0.001% was obtained for both compounds. However due to the bioassay-guided isolation strategy material was also lost during fraction testing, and real contents should be higher.

Infractopicrin (**1**): brown powder; UV (MeOH) λ_{max} (log ε) 208 (3.99), 263 (3.59), 321 (3.52), 371 (3.45), 387 (3.46); IR ν_{max} (diamond) 3670–3150, 3085, 1660, 1450, 1171, 1116, 799, 719 cm^{-1}; ^{1}H NMR and ^{13}C NMR data (see Table 3) are in agreement with published data;[9] LC–ESI-CIDMS (+30 eV), *m/z* 261 $[M]^+$ (100), 259 (2), 246 (3), 233 (25), 218 (6); ESI-FTICR-MS *m/z* 261.10242 (calcd for $C_{17}H_{13}N_2O^+$ 261.10224).

10-Hydroxy-infractopicrin (**2**): yellow powder; UV (MeOH) λ_{max} (log ε) 208 (4.23), 239 (3.76), 289 (3.70), 315 (3.47), 327 (3.49), 350 (3.35), 367 (3.49), 386 (3.46); IR ν_{max} (diamond) 3670–3150, 1674, 1205, 1182, 1132, 1022, 801, 723 cm^{-1}; ^{1}H NMR and ^{13}C NMR data: see Table 3; LC–ESI-CIDMS (+30 eV) *m/z* 277 (100), 275 (2), 262 (3), 249 (22), 233 (35), 221 (14). ESI-FTICR-MS: *m/z* 277.09745 (calcd for $C_{17}H_{13}N_2O_2^+$, 277.09715).

3.5. Bioassay for AChE inhibition

AChE from bovine erythrocytes was obtained from Sigma–Aldrich. Enzyme activity was measured using a 96-well microplate reader (Tecan) based on Ellman's method[10] as outlined by Rhee et al.[19] Additionally, to evaluate the BChE inhibition, equine serum BChE and synthetic butyrylthiocholine as substrate were used according to a previously described method.[19] All tests were performed as triplicates. Tacrine, physostigmine, and galanthamine (Sigma Aldrich) were used as references at concentrations up to 100 μM.

3.6. Bioassay for inhibition of fibril formation (Thioflavin T assay)

ThT assay was carried out according to Schilling et al.[20] Briefly, for preparation of a seedless peptide stock, Aβ1-40 was dissolved in hexafluoroisopropanol (HFIP) to a final concentration of 1 mM and incubated for at least 2 h at room temperature. The peptide concentration was determined by absorption at λ = 280 nm, using an extinction coefficient of 1490 M^{-1} cm^{-1}. Prior to use, the HFIP was evaporated and the peptide was dissolved in 0.1 M NaOH, filled up with phosphate buffered saline (PBS) and the solution neutralized by the addition of 0.1 M HCl, resulting in a peptide concentration of 100 μM. The volume of HCl/NaOH-solution was 10% of total volume. Compounds **1** and **2** were dissolved in DMSO and diluted using PBS to a final concentration of 100 μM containing 5% DMSO. 50 μl of Aβ1-40 solution were mixed with 50 μl substance solution and 100 μl of a solution of Thioflavin T in water (40 μM, 0.01% NaN_3) in a 96-well blackwell microplate. The plate was covered with an adhesive film and incubated in a plate reader at 37 °C. Fluorescence readings for recording the aggregation process were taken every 2 h for up to two weeks (λ_{exc} = 440 nm; λ_{emm} = 490 nm). Routinely, assays were performed in four cavities of one plate and the mean of the determined fluorescence units was calculated. For the investigation of AChE induced aggregation AChE from *Electrophorus electricus* (Sigma Aldrich) was added to the assay mixture (250 nM).

To investigate the quenching of ThT fluorescence by compounds **1** and **2**, mature fibrils of Aβ1-40 (25 μM) in ThT solution (20 μM) were incubated with the compounds (25 μM). The resulting fluorescence was measured and compared with the fluorescence readings without the compounds.

3.7. Cytotoxicity assay

Cytotoxicity was tested using the CytoTox-ONE homogenous membrane integrity assay (Promega) according to the manufacturer's protocol. The purpose of the assay was to evaluate the leakage of lactate dehydrogenase (LDH) from HepG2 as well as SH-SY5Y cells (both obtained from DSMZ, Braunschweig, Germany) after treatment with compounds **1** and **2** in two different concentrations (10 μM and 100 μM; $n = 3$).

3.8. Molecular modeling

X-ray structures of human BChE (PDB entry 1P0I) and of AChE from *Torpedo californica* complexed with butyrylcholine and (−)-huperzine A (PDB entry 2ACE), respectively, have been used for docking studies. Hydrogen atoms were included automatically by the use of the 3D-protonate option in MOE.[16] Docking studies were performed with GOLD version 3.2 with rigid proteins.[21–23] Alternatively, flexible side chain docking with PLANTS was performed.[24] The following side chains were allowed to be flexible for BChE during docking with PLANTS: Ser198, Asp70, Trp82, His438, Tyr332, Phe329, Thr120, Glu197, Tyr128 and Ile442. In case of AChE, Ser200, Asp72, Trp84, His440, Tyr334, Phe331, Ser122, Glu199, Tyr130, Ile444 were flexible. In all cases 30 docking arrangements were calculated for each compound. Docking results were visualized and analyzed with MOE. Molecular graphics were drawn using PyMOL.[25]

Acknowledgments

The authors would like to thank M. Süße and A. Denkert (IPB, Halle) for technical support. Professor Dr. H.-U. Demuth, Dr. S. Schilling and S. Wendler (Probiodrug AG, Halle) are gratefully acknowledged for providing the ThT- and cytotoxicity assay. E. Ludwig (Berlin) is kindly acknowledged for providing the water color picture of *Cortinarius infractus* depicted in the graphical abstract.

Supplementary data

Supplementary data (FT-ICR-HRESIMS spectrum and ^{1}H, ^{13}C NMR, HPLC chromatogram of compound **2**) associated with this article can be found, in the online version, at doi:10.1016/j.bmc.2010.01.074.

References and notes

1. Bartus, R. T.; Dean, R. L.; Beer, B.; Lippa, A. S. *Science* **1982**, *217*, 408.
2. Inestrosa, N. C.; Sagal, J. P.; Colombres, M. In *Alzheimer's Disease: Cellular and Molecular Aspects of Amyloid β*; Harris, R., Fahrenholz, F., Eds.; Springer: New York, 2005; Vol. 38, pp 299–317.
3. Inestrosa, N. C.; Alvarez, A.; Perez, C. A.; Moreno, R. D.; Vicente, M.; Linker, C.; Casanueva, O. I.; Soto, C.; Garrido, J. *Neuron* **1996**, *16*, 881.
4. Melzer, D. *BMJ* **1998**, *316*, 762.
5. Schulz, V. *Phytomedicine* **2003**, *10*, 74.
6. Mueller, G. M.; Schmit, J. P. *Biodivers. Conserv.* **2007**, *16*, 1.
7. Liu, J. K. *Chem. Rev.* **2005**, *105*, 2723.
8. Gill, M.; Steglich, W. *Pigments of Fungi (Macromycetes)*; Springer: Wien, New York, 1987.
9. Steglich, W.; Kopanski, L.; Wolf, M.; Tegtmeyer, G. *Tetrahedron Lett.* **1984**, *25*, 2341.
10. Ellman, G. L.; Courtney, K. D.; Andres, V., Jr.; Featherstone, R. M. *Biochem. Pharmacol.* **1961**, *7*, 88.
11. Thomsen, T.; Kewitz, H. *Life Sci.* **1990**, *46*, 1553.
12. Becher, P. G.; Beuchat, J.; Gademann, K.; Juttner, F. *J. Nat. Prod.* **2005**, *68*, 1793.
13. Becher, P. G.; Baumann, H. I.; Gademann, K.; Juttner, F. *J. Appl. Phycol.* **2009**, *21*, 103.
14. Schott, Y.; Decker, M.; Rommelspacher, H.; Lehmann, J. *Bioorg. Med. Chem. Lett.* **2006**, *16*, 5840.
15. Ghosal, S.; Bhattacharya, S. K.; Mehta, R. *J. Pharm. Sci.* **1972**, *61*, 808.
16. Chemical Computing Group Inc. MOE (The Molecular Operating Environment) **2007** Vers. 2007.09.
17. Lipinski, C. A.; Lombardo, F.; Dominy, B. W.; Feeney, P. J. *Adv. Drug Delivery Rev.* **1997**, *23*, 3.
18. Ertl, P.; Rohde, B.; Selzer, P. *J. Med. Chem.* **2000**, *43*, 3714.
19. Rhee, I. K.; van de Meent, M.; Ingkaninan, K.; Verpoorte, R. *J. Chromatogr., A* **2001**, *915*, 217.
20. Schilling, S.; Lauber, T.; Schaupp, M.; Manhart, S.; Scheel, E.; Bohm, G.; Demuth, H. U. *Biochemistry* **2006**, *45*, 12393.
21. Jones, G.; Willett, P.; Glen, R. C.; Leach, A. R.; Taylor, R. *J. Mol. Biol.* **1997**, *267*, 727.
22. Nissink, J. W. M.; Murray, C.; Hartshorn, M.; Verdonk, M. L.; Cole, J. C.; Taylor, R. *Proteins* **2002**, *49*, 457.
23. Verdonk, M. L.; Cole, J. C.; Hartshorn, M. J.; Murray, C. W.; Taylor, R. D. *Proteins* **2003**, *52*, 609.
24. Korb, O.; Stützle, T.; Exner, T. *Swarm Intell.* **2007**, *1*, 115.
25. DeLano Scientific LLC. The PyMOL Molecular Graphics System **2008** Vers. 1.1.